INORGANIC CHEMISTRY
FRONTIERS

RESEARCH ARTICLE

View Article Online
View Journal | View Issue

Cite this: *Inorg. Chem. Front.*, 2017, **4**, 1182

Self-sacrificed two-dimensional REO(CH_3COO) template-assisted synthesis of ultrathin rare earth oxide nanoplates†

Rui Liu, Ke Wu, Lin-Dong Li, Ling-Dong Sun and Chun-Hua Yan *

Received 14th April 2017,
Accepted 17th May 2017

DOI: 10.1039/c7qi00201g

rsc.li/frontiers-inorganic

In this Communication, a general two-dimensional (2D) template method for the synthesis of ultrathin 2D nanomaterials of non-layered compounds is reported. With this method, the whole series of ultrathin rare earth oxide (RE_2O_3) nanoplates are synthesized by using *in situ* formed REO(CH_3COO) nanoplates as self-sacrificed templates.

The synthesis and application of an ultrathin 2D nanostructure is a research area attracting ever-increasing attention since the discovery of graphene by Novoselov and Geim in 2004.[1–3] Compared with their bulk counterpart, ultrathin 2D nanomaterials with a thickness less than 5 nm show many unique properties thanks to their high specific area, abundant surface defects and strong quantum confinement of electrons, and have been investigated as functional materials with promising applications in high efficiency catalysis, nanodevices, Li-ion batteries, supercapacitors, photodetectors and high efficiency cooling technologies.[4–10] To date, a lot of methods have been devised for the synthesis of ultrathin 2D nanomaterials of layered compounds, typically by delamination of layered compounds with mechanical exfoliation and/or ion/surfactant insertion and chemical vapour decomposition (CVD).[6] For non-layered compounds, the lack of an intrinsic driving force for 2D growth makes the preparation quite challenging and is usually based on trial-and-error which greatly reduces the research efficiency.[4,7,8] Therefore, a rational and general synthesis method for ultrathin 2D nanomaterials of non-layered compounds is highly desired. In recent years, a self-sacrificed template method is widely used for the synthesis of 1D[11] and 2D[12,13] nanostructures. Considering the great variety of layered compounds and previously reported ultrathin 2D nanomaterials, taking the as-synthesized ultrathin 2D nanomaterials as self-sacrificed templates to synthesize ultrathin 2D nanomaterials of non-layered compounds will be a promising method.[14–19]

Beijing National Laboratory for Molecular Sciences, State Key Laboratory of Rare Earth Materials Chemistry and Applications, PKU-HKU Joint Laboratory in Rare Earth Materials and Bioinorganic Chemistry, College of Chemistry and Molecular Engineering, Peking University, Beijing 100871, China. E-mail: yan@pku.edu.cn

†Electronic supplementary information (ESI) available: Synthesis details and supplementary figures. See DOI: 10.1039/c7qi00201g

RE_2O_3 are a series of typical non-layered compounds. Compared with bulk RE_2O_3, ultrathin 2D RE_2O_3 nanomaterials have shown obvious performance enhancement and many new properties in catalysis,[20,21] photonics[22] and magnetics.[23,24] The preparation of ultrathin RE_2O_3 nanoplates has gained great achievement in the past decade, while some challenges still exist. Cao reported the first synthesis of ultrathin RE_2O_3 nanoplates, square Gd_2O_3 nanoplates, by a heat-up pyrolysis method in 2004.[25] After that, our group and other groups devised similar heat-up pyrolysis methods, solvothermal methods and digestive ripening methods for the synthesis of the whole series of ultrathin RE_2O_3 nanoplates.[20–34] Although many synthesis methods have been reported, two main problems still exist. First, a more general method for the synthesis of the whole series of ultrathin RE_2O_3 nanoplates is still needed because each of the aforementioned synthesis methods could be only used to synthesize limited kinds of RE_2O_3 nanoplates. Second, the exact 2D growth mechanism of ultrathin RE_2O_3 nanoplates by the aforementioned methods is still unclear. The vague 2D growth mechanism has restrained further study and is a pressing problem to be resolved.

To address these challenges, we designed a self-sacrificed template method for the synthesis of ultrathin RE_2O_3 nanoplates with rare earth oxide acetate (REO(CH_3COO)) nanoplates as templates. Based on the design, a novel hot-injection pyrolysis method for the synthesis of the whole series of ultrathin RE_2O_3 nanoplates is hereby reported. *In situ* formed single-layered (SL) and multi-layered (ML) REO(CH_3COO) nanoplates are used as self-sacrificed templates to mediate the synthesis of ultrathin SL and ML RE_2O_3 nanoplates, respectively. This self-sacrificed template method is robust and general, and provides the foundation for further research on the controlled synthesis of ultrathin RE_2O_3 nanomaterials.

In the synthesis process, the ultrathin RE_2O_3 nanoplates are formed by two successive pyrolysis reactions. At first, SL or ML

REO(CH_3COO) nanoplates are formed by injecting the oleic acid (OA) and oleylamine (OAm) solution of rare earth acetate into the mixture of OA and OAm at 310 °C under a N_2 atmosphere. Then ultrathin RE_2O_3 nanoplates are formed by further pyrolysis of the as-synthesized REO(CH_3COO) nanoplates.

REO(CH_3COO) is chosen as the self-sacrificed template mainly due to two reasons. First, REO(CH_3COO) is a probable layered compound which is prone to forming a 2D nanostructure. Although there has been no crystal structure available for REO(CH_3COO) so far, REOX (X = Cl^-, Br^-, I^-, $1/2CO_3^{2-}$, $1/2SO_4^{2-}$) has long been known to have a layered structure as shown in Fig. S1.† [35–38] In REOX, RE-O layers are formed by strong ionic bonds, and sandwiched between two X layers. Because of the oxophilicity of lanthanide elements, X ions such as Br^- can be easily substituted by carboxylate ions with the 2D structure maintaining.[39] Second, REO(CH_3COO) is the pyrolysis intermediate of rare earth acetates, and they can transform into the corresponding RE_2O_3 by further pyrolysis reaction.[40–52]

The as-synthesized REO(CH_3COO) nanoplates all have similar morphology. Taking CeO(CH_3COO) nanoplates as an example, transmission electron microscopy (TEM) images (Fig. 1a, b and S2†) show a plate-like morphology, and the X-ray diffraction (XRD) pattern (Fig. 1c) matches well with that of CeO(CH_3COO) reported in the literature.[37,48] Time sequence experiments are conducted during the synthesis to illustrate the growth behavior. The synthesis begins after the hot injection, at about 1 min after the injection, the preliminary products are mainly nanodots and worm-like nanorods with low crystallinity (Fig. 2a). Two minutes later, the products have mostly grown into CeO(CH_3COO) SL nanoplates with irregular shapes (Fig. 2b and S3†). At 5 min after the injection, rectangular CeO(CH_3COO) SL nanoplates have formed, and the contrast difference in the nanoplates shows that they have started to grow layer-by-layer (Fig. 2c and S3†). ML nanoplates as shown in Fig. 2d emerge at about 10 min after the injection. TEM and XRD characterization of the time sequence samples shows that CeO(CH_3COO) SL nanoplates are first formed in the synthesis process and then gradually grow into the CeO(CH_3COO) ML nanoplates through a layer-by-layer growth pattern.

During the synthesis of the CeO(CH_3COO) nanoplates, when the CeO(CH_3COO) SL nanoplates are formed, typically at 3 min after the injection, adding a mixture of 3 mmol OA and 9 mmol OAm into the reaction system will restrain the layer-by-layer growth and the as-synthesized CeO(CH_3COO) SL nanoplates can transform into ceria SL nanoplates without elevating the reaction temperature (see the ESI† for details). TEM images of the as-synthesized ceria SL nanoplates are shown in Fig. 3. Fig. 3a shows that the SL nanoplates have a length of 177 ± 12 nm and a width of 17 ± 2 nm. Fig. 3b and the inset show that the SL nanoplates have a thickness of 1.1 ± 0.2 nm. The Fourier transform infrared (FT-IR) spectrum (Fig. S4a†) shows that the as-synthesized SL nanoplates are covered by oleate ions. The small-angle XRD (SAXRD) pattern (Fig. S4b†) of the SL nanoplates shows obvious (001) and (002) reflections at 2.9° and 5.4°, respectively, which indicates the arrangement of the nanoplates with a periodicity of 3.0 nm. These results fit well with the thickness of the nanoplates measured from TEM

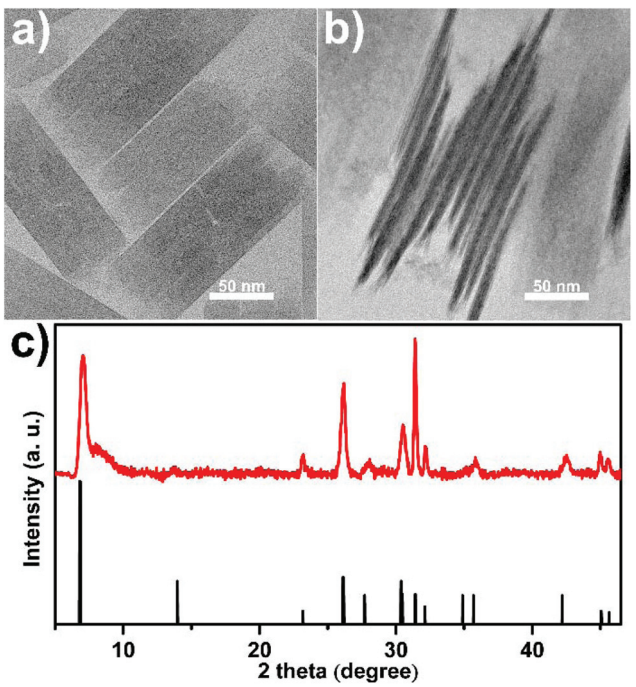

Fig. 1 (a, b) TEM images and (c) XRD pattern of the as-synthesized CeO(CH_3COO) ML nanoplates, the reference pattern in (c) is produced from ref. 41 and 52.

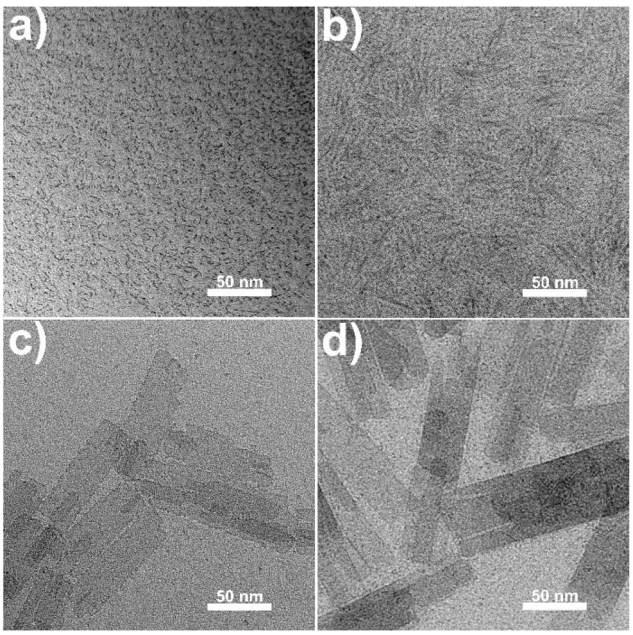

Fig. 2 TEM images of products obtained at (a) 1 min, (b) 3 min, (c) 5 min and (d) 10 min after injection during the synthesis of CeO(CH_3COO) ML nanoplates.

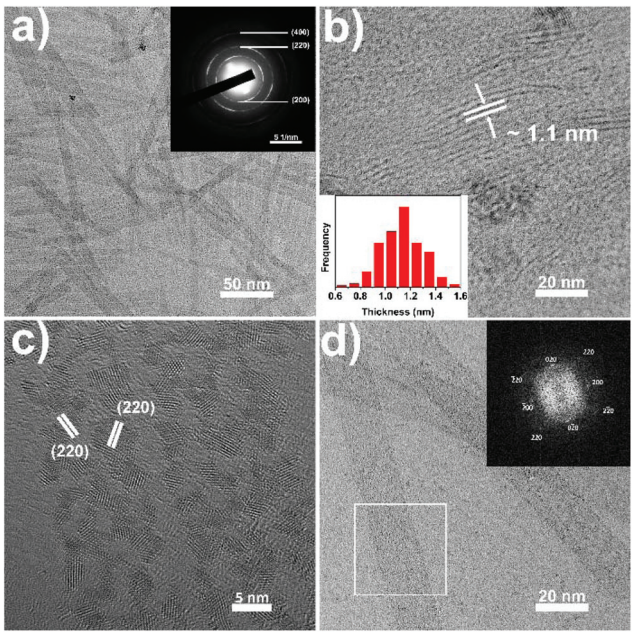

Fig. 3 Characterization of the as-synthesized ceria SL-nanoplates. (a, b) TEM images; (c) HRTEM image; (d) TEM images; the inset in (a) is the SAED pattern of the ceria SL-nanoplates; the inset in (b) shows the thickness distribution of the SL-nanoplates; the inset in (d) is the FFT pattern of the selected area in (d).

images as the length of 1.8 nm for oleate ions (Fig. S4b†). The selected area electron diffraction (SAED) pattern (inset in Fig. 3a) and high-resolution TEM (HRTEM) image (Fig. 3c), together with the XRD pattern (Fig. S5†), confirm that the SL nanoplates are ceria (JCPDS no. 04-0593) with a cubic fluorite structure. Due to the ultrathin nature of the ceria SL nanoplates, they are fragmentized under high-energy electron beam irradiation preventing the confirmation of the exposure facets of the SL nanoplates from the HRTEM image. Fig. 3d is taken at a much smaller magnification of 200k, and the fast Fourier transform (FFT) pattern (inset in Fig. 3d) of the selected area in Fig. 3d shows an array of spots which can be indexed to the {200} and {220} reflections of ceria. The FFT pattern clearly indicates that the SL nanoplates are single crystals, and enclosed with {100} facets.[5]

During the synthesis of $CeO(CH_3COO)$ nanoplates, when the ML nanoplates are formed, typically at 10 min after the injection, raising the reaction temperature to 380 °C will lead to the formation of ceria ML nanoplates with $Ce_2O_2CO_3$ ML nanoplates as an intermediate (Fig. S6†) (see the ESI† for details). TEM images of ceria ML nanoplates are shown in Fig. 4. Fig. 4a and b (also see Fig. S7†) show that the as-synthesized ceria ML nanoplates have a 2D lamellar structure in which many ultrathin layers stack together. The high-angle annular dark-field scanning TEM (HAADF-STEM) image of the product (Fig. 4c) shows an obvious contrast difference in each nanoplate and further confirms the multi-layered structure. The ML nanoplates have a width of 46 ± 8 nm, a length of 166 ± 30 nm and a total thickness of 7 ± 2 nm. The XRD

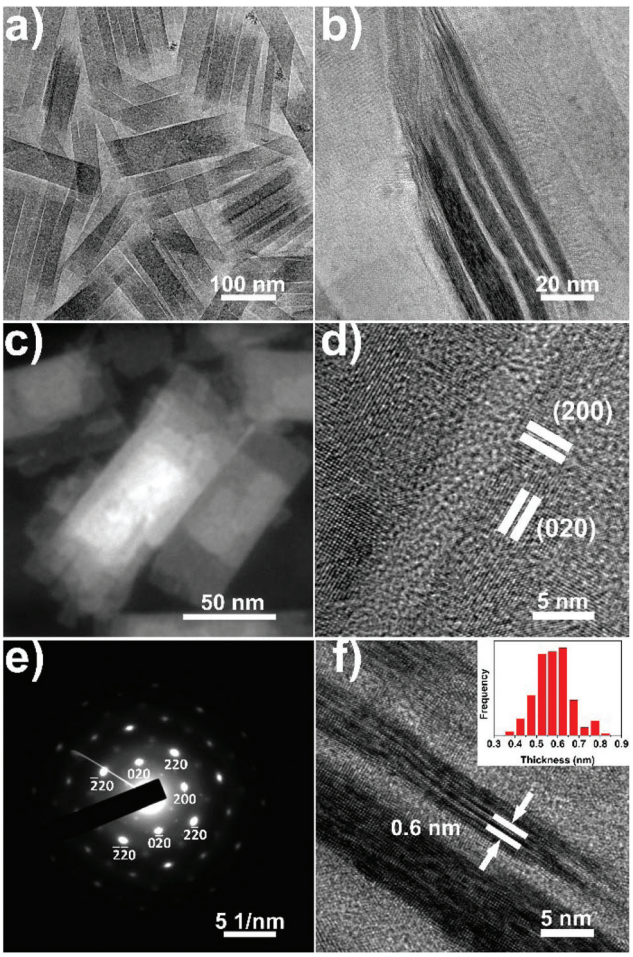

Fig. 4 Characterization of the as-synthesized ceria ML-nanoplates. (a, b) TEM images; (c) HAADF-STEM image; (e) SAED pattern; (d, f) HRTEM images; the inset in (f) shows the thickness distribution of the layers in the ML nanoplates.

pattern of the ML nanoplates (Fig. S8†) can be well indexed to ceria (JCPDS no. 04-0593). The HRTEM image of the ceria ML nanoplates (Fig. 4d) shows an interplanar distance of 0.28 nm along both the long and short edges of the rectangular nanoplates, indicating that the four sides of the ceria ML nanoplates are all {100} facets. The SAED pattern (Fig. 4e) shows that ceria ML nanoplates are single crystals, and the zone axis is [001] which indicates that both the top and bottom surfaces of the nanoplates belong to the {100} facets. In the XRD pattern (Fig. S8†), the (200) peak is the strongest peak. The unusual high intensity indicates that the as-synthesized ceria ML nanoplates expose more (200) facets which is consistent with the HRTEM and SAED results. TEM images taken from the side of the ML nanoplates (Fig. 4f and S7†) show that the layers in the ML nanoplates have a thickness of 0.6 ± 0.1 nm, which is approximately the size of a single ceria unit cell (0.54 nm). The thickness is smaller than that of the SL nanoplates which can be explained by the multi-layered structure restraining the growth of the layers in the ML nanoplates.

From the above experiments, we could see that CeO(CH_3COO) plays a critical role in the synthesis of ceria ML and SL nanoplates. As a pyrolysis intermediate of cerium acetate, it acts as the *in situ* formed self-sacrificed template for the preparation of ceria SL and ML nanoplates by the hot-injection pyrolysis method. With similar reaction conditions to the synthesis of their cerium counterpart (see the ESI† for details), the whole series of REO(CH_3COO) ML nanoplates (Fig. S9†) are formed. Fig. S9† shows that the as-synthesized REO (CH_3COO) nanoplates all adopt a ML plate-like morphology with a lateral size ranging from 100 nm to several microns. XRD results (Fig. S10†) show that they all crystallize in the same structure as CeO(CH_3COO). By introducing extra OA and OAm into the reaction system, the whole series of RE_2O_3 SL nanoplates are formed (Fig. S11†). The RE_2O_3 SL nanoplates are rectangular from La_2O_3 to Eu_2O_3, and circular from Gd_2O_3 to Lu_2O_3 and Y_2O_3. XRD results (Fig. S12†) also show a similar transformation with the strongest peak transforming from (004) to (111). The HRTEM images of the SL Eu_2O_3, Gd_2O_3 and Y_2O_3 nanoplates in Fig. S13† show the exposed facets transformed from {004} to {111}.

In summary, we have constructed a self-sacrificed template method for the synthesis of the whole series of ultrathin rare earth oxide nanoplates with *in situ* formed REO(CH_3COO) nanoplates that act as the template. The self-sacrificed template method is robust and general, and provides the foundation for further research on ultrathin rare earth oxide nanoplates.

Acknowledgements

This work was supported by the NSFC (No. 21425101, 21321001, 21371011, 21331001, and 91422302) and the MOST of china (2014CB643800).

References

1 K. S. Novoselov, A. K. Geim, S. V. Morozov, D. Jiang, Y. Zhang, S. V. Dubonos, I. V. Grigorieva and A. A. Firsov, *Science*, 2004, **306**, 666–669.
2 K. J. Koski and Y. Cui, *ACS Nano*, 2013, **7**, 3739–3744.
3 S. Z. Butler, S. M. Hollen, L. Y. Cao, Y. Cui, J. A. Gupta, H. R. Gutierrez, T. F. Heinz, S. S. Hong, J. X. Huang, A. F. Ismach, E. Johnston-Halperin, M. Kuno, V. V. Plashnitsa, R. D. Robinson, R. S. Ruoff, S. Salahuddin, J. Shan, L. Shi, M. G. Spencer, M. Terrones, W. Windl and J. E. Goldberger, *ACS Nano*, 2013, **7**, 2898–2926.
4 X. Zhang and Y. Xie, *Chem. Soc. Rev.*, 2013, **42**, 8187–8199.
5 Y. Guo, K. Xu, C. Wu, J. Zhao and Y. Xie, *Chem. Soc. Rev.*, 2015, **44**, 637–646.
6 M. Chhowalla, H. S. Shin, G. Eda, L. J. Li, K. P. Loh and H. Zhang, *Nat. Chem.*, 2013, **5**, 263–275.
7 C. Tan and H. Zhang, *Nat. Commun.*, 2015, **6**, 7873.
8 S. Hu and X. Wang, *Chem. Soc. Rev.*, 2013, **42**, 5577–5594.
9 H. Zhang, *ACS Nano*, 2015, **9**, 9451–9469.
10 C. Tan and H. Zhang, *Chem. Soc. Rev.*, 2015, **44**, 2713–2731.
11 H. X. Mai, L. D. Sun, Y. W. Zhang, R. Si, W. Feng, H. P. Zhang, H. C. Liu and C. H. Yan, *J. Phys. Chem. B*, 2005, **109**, 24380–24385.
12 Q. Dai, S. Bai, H. Li, W. Liu, X. Wang and G. Lu, *CrystEngComm*, 2014, **16**, 9817–9827.
13 Q. Dai, W. Wang, X. Wang and G. Lu, *Appl. Catal., B*, 2017, **203**, 31–42.
14 W. Bi, M. Zhou, Z. Ma, H. Zhang, J. Yu and Y. Xie, *Chem. Commun.*, 2012, **48**, 9162–9164.
15 Y. Sun, Q. Liu, S. Gao, H. Cheng, F. Lei, Z. Sun, Y. Jiang, H. Su, S. Wei and Y. Xie, *Nat. Commun.*, 2013, **4**, 2899.
16 F. Lei, Y. Sun, K. Liu, S. Gao, L. Liang, B. Pan and Y. Xie, *J. Am. Chem. Soc.*, 2014, **136**, 6826–6829.
17 X. J. Wu, X. Huang, X. Qi, H. Li, B. Li and H. Zhang, *Angew. Chem., Int. Ed.*, 2014, **53**, 8929–8933.
18 X. J. Wu, X. Huang, J. Liu, H. Li, J. Yang, B. Li, W. Huang and H. Zhang, *Angew. Chem., Int. Ed.*, 2014, **53**, 5083–5087.
19 Y. Zhu, C. Cao, T. Shi, W. Chu, Z. Wu and Y. Li, *Sci. Rep.*, 2014, **4**, 5787–5787.
20 D. Wang, Y. Kang, V. Doan-Nguyen, J. Chen, R. Küngas, N. L. Wieder, K. Bakhmutsky, R. J. Gorte and C. B. Murray, *Angew. Chem., Int. Ed.*, 2011, **50**, 4378–4381.
21 D. Wang, Y. Kang, X. Ye and C. B. Murray, *Chem. Mater.*, 2014, **26**, 6328–6332.
22 D. Hudry, A. M. M. Abeykoon, J. Hoy, M. Y. Sfeir, E. A. Stach and J. H. Dickerson, *Chem. Mater.*, 2015, **27**, 965–974.
23 Q. Zhang and B. Yan, *Chem – Eur. J.*, 2012, **18**, 5150–5154.
24 T. Paik, T. R. Gordon, A. M. Prantner, H. Yun and C. B. Murray, *ACS Nano*, 2013, **7**, 2850–2859.
25 Y. C. Cao, *J. Am. Chem. Soc.*, 2004, **126**, 7456–7457.
26 R. Si, Y. W. Zhang, L. P. You and C. H. Yan, *Angew. Chem., Int. Ed.*, 2005, **44**, 3256–3260.
27 R. Si, Y. W. Zhang, H. P. Zhou, L. D. Sun and C. H. Yan, *Chem. Mater.*, 2006, **19**, 18–27.
28 T. Yu, J. Joo, Y. I. Park and T. Hyeon, *J. Am. Chem. Soc.*, 2006, **128**, 1786–1787.
29 J. Jeong, N. Kim, M. G. Kim and W. Kim, *Chem. Mater.*, 2016, **28**, 172–179.
30 Z. Huo, C. K. Tsung, W. Huang, M. Fardy, R. Yan, X. Zhang, Y. Li and P. Yang, *Nano Lett.*, 2009, **9**, 1260–1264.
31 S. Hu, H. Liu, P. Wang and X. Wang, *J. Am. Chem. Soc.*, 2013, **135**, 11115–11124.
32 H. Imagawa and S. Sun, *J. Phys. Chem. C*, 2012, **116**, 2761–2765.
33 X. Zhang, J. Ge, Y. Xue, B. Lei, D. Yan, N. Li, Z. Liu, Y. Du and R. Cai, *Chem – Eur. J.*, 2015, **21**, 11954–11960.
34 X. Y. Zhang, Y. W. Wang, F. H. Cheng, Z. P. Zheng and Y. P. Du, *Sci. Bull.*, 2016, **18**, 1422–1434.
35 J. Höls, M. Lahtinen, M. Lastusaari, J. Valkonen and J. Viljanen, *J. Solid State Chem.*, 2002, **165**, 48–55.
36 R. P. Turcotte, J. O. Sawyer and L. R. Eyring, *Inorg. Chem.*, 1969, **8**, 238–246.

37 H. Hülsing, H. G. Kahle, M. Schwab and H. J. Schwarzbauer, *J. Magn. Magn. Mater.*, 1978, **9**, 68–70.
38 D. Yan, B. Lei, X. J. Wu, Z. Q. Liu, N. Li, J. Ge, Y. M. Xue, Y. P. Du, Z. P. Zheng and H. Zhang, *Appl. Mater. Today*, 2015, **1**, 20–26.
39 L. Zhang, D. Jiang, J. Xia, C. Li, N. Zhang and Q. Li, *RSC Adv.*, 2014, **4**, 17648–17652.
40 M. Inoue, H. Kominami, H. Otsu and T. Inui, *Nippon Kagaku kaishi*, 1991, **1991**, 1254–1260.
41 H. Kominami, M. Inoue and T. Inui, *Nippon Kagaku kaishi*, 1993, **1993**, 605–611.
42 S. Hosokawa, S. Iwamoto and M. Inoue, *Mater. Res. Bull.*, 2008, **43**, 3140–3148.
43 S. Hosokawa, K. Shimamura and M. Inoue, *Mater. Res. Bull.*, 2011, **46**, 1928–1932.
44 K. Manabe, M. Ogawa and Y. Eizuka, *Nippon Kagaku kaishi*, 1983, 461–463.
45 K. Manabe and M. Ogawa, *Nippon Kagaku kaishi*, 1979, 1013–1019.
46 M. Ogawa and K. Manabe, *Nippon Kagaku kaishi*, 1993, 600–604.
47 M. Ogawa and K. Manabe, *J. Ceram. Soc. Jpn.*, 1988, **96**, 890–893.
48 K. Manabe and M. Ogawa, *Nippon Kagaku kaishi*, 1982, 694–696.
49 M. Ogawa and K. Manabe, *J. Ceram. Soc. Jpn.*, 1988, **96**, 672–676.
50 T. Arii, A. Kishi, M. Ogawa and Y. Sawada, *Anal. Sci.*, 2001, **17**, 875–880.
51 T. Arii, T. Taguchi, A. Kishi, M. Ogawa and Y. Sawada, *J. Eur. Ceram. Soc.*, 2002, **22**, 2283–2289.
52 K. Manabe and M. Ogawa, *Nippon Kagaku kaishi*, 1983, **1983**, 1092–1095.